Ultra-high-speed 300-GHz InP IC Technology for Beyond 5G

Hiroshi Hamada, Takuya Tsutsumi, Hideaki Matsuzaki, Hiroki Sugiyama, and Hideyuki Nosaka

Abstract

A 300-GHz-band 120 Gbit/s wireless transceiver (TRX) is presented using our in-house indium phosphide (InP) high-electron-mobility transistor (InP-HEMT) technology. A 300-GHz power amplifier (PA), which is the key component in the TRX, was developed using the backside DC line (BDCL) technique to increase its gain and output power. The measured maximum gain and saturated output power are respectively 20.5 dB and 12 dBm. The 300-GHz-band TRX was fabricated using this PA. The TRX achieves high data rates of 124 and 120 Gbit/s under back-to-back and 9.8-m-link-distance wireless data transmission conditions. To the best of our knowledge, these are the highest data rates among reported 300-GHz-band TRXs.

Keywords: 300 GHz, InP-HEMT, power amplifier

1. Introduction

A terahertz (THz) wave is an electromagnetic wave located in the boundary of a radio wave and light wave, as illustrated in **Fig. 1**. Its frequency range is from around 300 GHz to 10 THz. It had been very difficult to generate and control THz waves due to the lack of semiconductor devices working in this high frequency region. Due to the progress of miniaturization technique for semiconductor devices (transistors), the operation frequency range of cutting-edge transistors is above 1 THz [1]. By using these high-speed transistors, the applications of THz waves, such as wireless communication [2] and imaging/sensing for security [3], are being extensively investigated. High-speed wireless communication is one of the major applications of THz waves due to their broad bandwidth. In the next generation of the fifth-generation mobile communication system (5G), called beyond 5G or 6G, a data rate of more than 100 Gbit/s is considered necessary. The 300-GHz-band is considered suitable for beyond 5G due to its relatively low atmospheric attenuation (< 10 dB/km) in the THz region. In this article, we report on the recent achievements with a 300-GHz-band power amplifier (PA) we developed using our in-house indium phosphide (InP) high-electron-mobility transistor (InP-HEMT) integrated circuit (IC) technology and over-100 Gbit/s wireless transceiver front-end (TRX) fabricated using this PA.

2. InP-HEMT technologies

InP device technologies to fabricate 300-GHz-band ICs for TRXs are introduced in this section.

The mandatory device technology for 300-GHz-band ICs is the high-speed transistor InP-HEMT. There are two frequently used figures of merit for high-speed transistors, i.e., transition frequency (f_T) and maximum oscillation frequency (f_{MAX}). The former is an index to show the maximum switching speed and the latter shows the maximum power-amplification frequency of the transistor. Therefore, f_T is related to the operation frequency of a switching circuit such as a passive mixer and multiplier, whereas f_{MAX} is related to the operation frequency of active circuits such as an amplifier and oscillator. A cross-section schematic of our in-house InP-HEMT is shown in **Fig. 2(a)**. Generally, InP-HEMTs have superior high-speed characteristics by using the

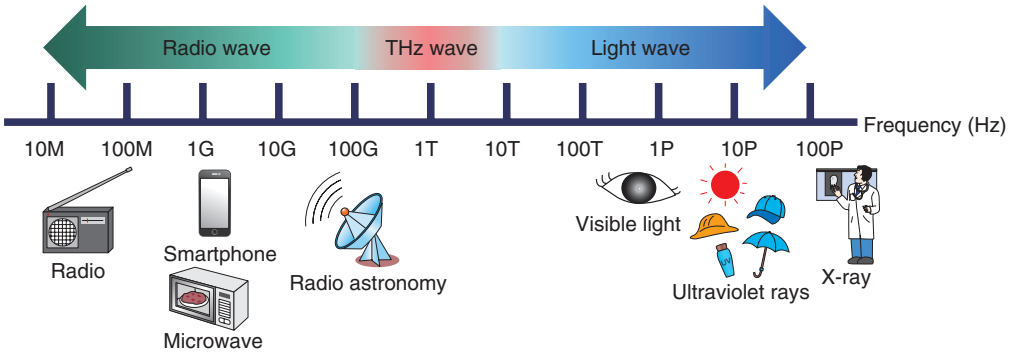

Fig. 1. THz wave.

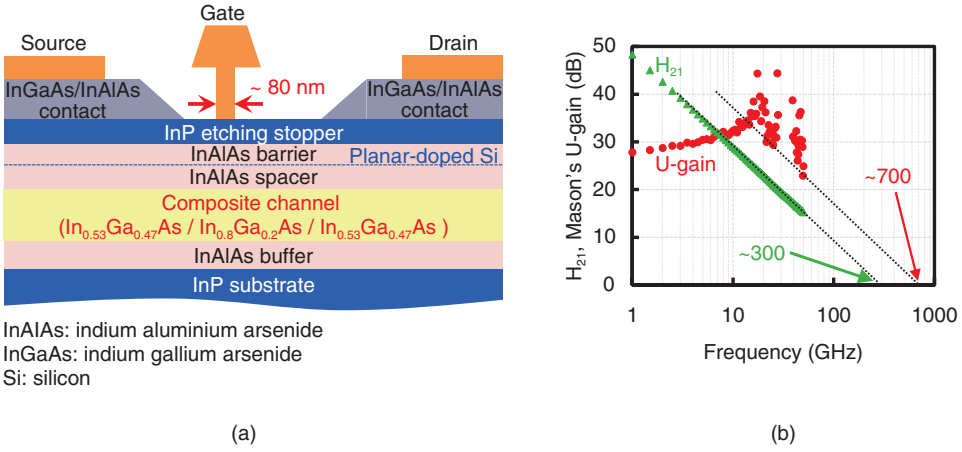

Fig. 2. (a) Schematic and (b) RF characteristics of in-house InP-HEMT.

high-electron-mobility material indium gallium arsenide ($In_{0.53}Ga_{0.47}As$), which can be epitaxially grown (i.e., lattice-matched with InP) on InP substrate as their channels. With our InP-HEMT technology, to attain higher speed than with normal InP-HEMTs, a composite channel composed of In-rich $In_{0.8}Ga_{0.2}As$ and lattice-matched $In_{0.53}Ga_{0.47}As$ [4] is applied using InGaAs because the ratio increase of In can enhance its electron mobility. The gate length also decreased to 80 nm to shorten the electron transit time in the channel and enhance both f_T and f_{MAX}. The measured current gain (H_{21}) and maximum unilateral gain (U-gain) of this InP-HEMT are plotted in **Fig. 2(b)**, showing high f_T and f_{MAX} of 300 and 700 GHz, respectively.

To fabricate 300-GHz-band ICs, it is not sufficient to have high-speed transistors. The problem specific to THz ICs caused by a substrate mode as described below should be managed. A substrate mode is an electromagnetic wave that propagates in substrate. When the substrate thickness is the same order of wavelength, the substrate mode can propagate. The commercially available InP substrate thickness is around 600 μm and the wavelength of a 300-GHz-band signal in InP substrate is below 500 μm. Therefore, a substrate mode can be guided, causing unwanted coupling between some ports of THz ICs, e.g., coupling of input and output ports of the amplifier by the substrate mode can cause the oscillation of that amplifier. To cut out the propagation of the substrate mode, substrate thinning and through substrate via (TSV) are applied in the back-end IC process [5, 6]. By using substrate thinning, the thickness of the InP substrate is reduced to 55 μm, as shown in **Fig. 3(a)**. TSVs are densely formed over the entire substrate area to reduce the substrate space that can

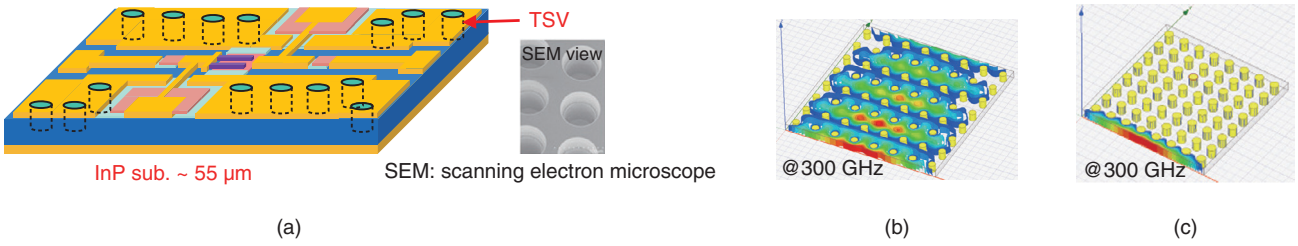

Fig. 3. (a) InP chip with substrate thinning and dense TSV formation, substrate-mode propagation for TSV pitches of (b) 100 μm and (c) 50 μm.

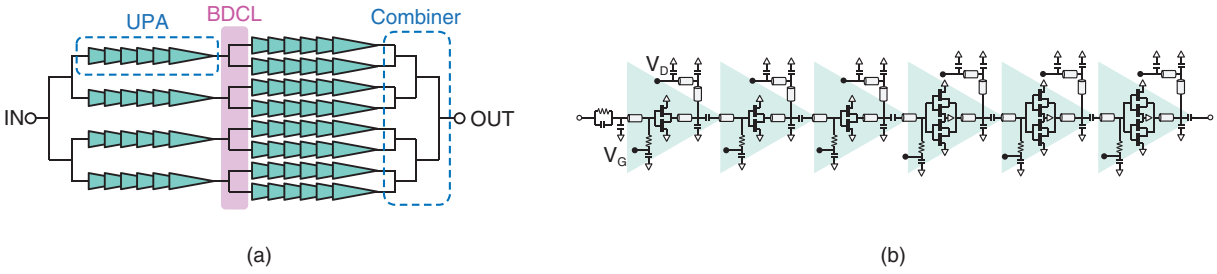

Fig. 4. Schematics of (a) 300-GHz PA and (b) UPA.

support the propagation of substrate modes, as also shown in Fig. 3(a). The TSV density is critical to sufficiently cut out the substrate mode. **Figures 3(b)** and **(c)** shows a 300-GHz substrate-mode propagation calculated using an electromagnetic simulator when the TSV pitch (TSV edge-to-edge distance) is set to 100 and 50 μm, respectively. By using the 50-μm pitch, the substrate mode is sufficiently cut out. Therefore, around the 50-μm pitch, the TSV layout is used in the 300-GHz-band PA, as described in the next section.

3. 300-GHz PA

The important characteristics of the PA for TRXs are gain and output power to achieve a sufficient signal-to-noise ratio (SNR) of 300-GHz-band wireless communication. A schematic of the PA is shown in **Fig. 4(a)**. It is composed of unit power amplifiers (UPAs) consisting of six-stage common-source amplifiers using the InP-HEMTs described in Section 2, as illustrated in **Fig. 4(b)**. This six-stage cascading design produces high gain of more than 10 dB for a UPA at 300 GHz. The inter-stage matching for each common-source amplifier stage in a UPA is designed to have small loss by using the low impedance matching technique [7, 8]. To achieve both high gain and high output power in a UPA, the first three stages are designed with high-gain two-fingered HEMTs, and the latter three stages are designed with four-fingered HEMTs that have higher power handling and slightly lower gain than two-fingered ones, as shown in Fig. 4(b). The PA has eight-paralleled UPAs in its output stage to achieve high output power by combining the output power of each UPA. In the middle part of the PA, the backside DC line (BDCL) is used to also achieve high gain and output power. The role of the BDCL technique is explained as follows.

The PA shown in Fig. 4 (a) uses many transistors due to the series-amplifier stage in a UPA and paralleled fashion in the PA output stage. In such a case, a very wide (several hundred microns) DC line should be used to support large total drain current (~ 1.8 A), which is necessary to operate many transistors. Therefore, the typical layout of this PA is similar to the one shown in **Fig. 5(a)**. Long radio frequency (RF) transmission lines (TLs) should overlap the wide DC line. These long RF TLs have high transmission loss in a high frequency range, such as the 300-GHz band, and reduce the gain and output power of the PA. To address this issue, the BDCL is introduced. With this introduction, the wide DC line is put on the

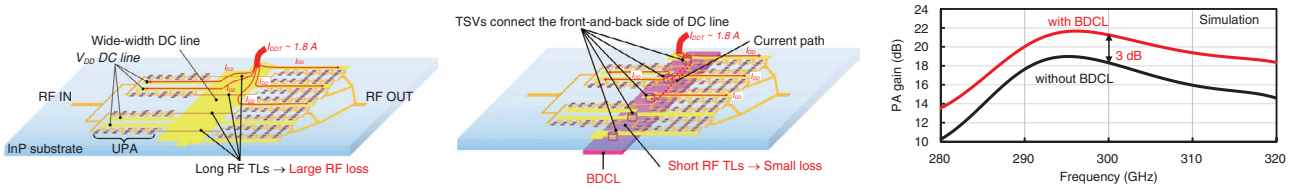

Fig. 5. Layout schematics of 300-GHz PA (a) without and (b) with BDCL and (c) PA gain comparison of these layouts.

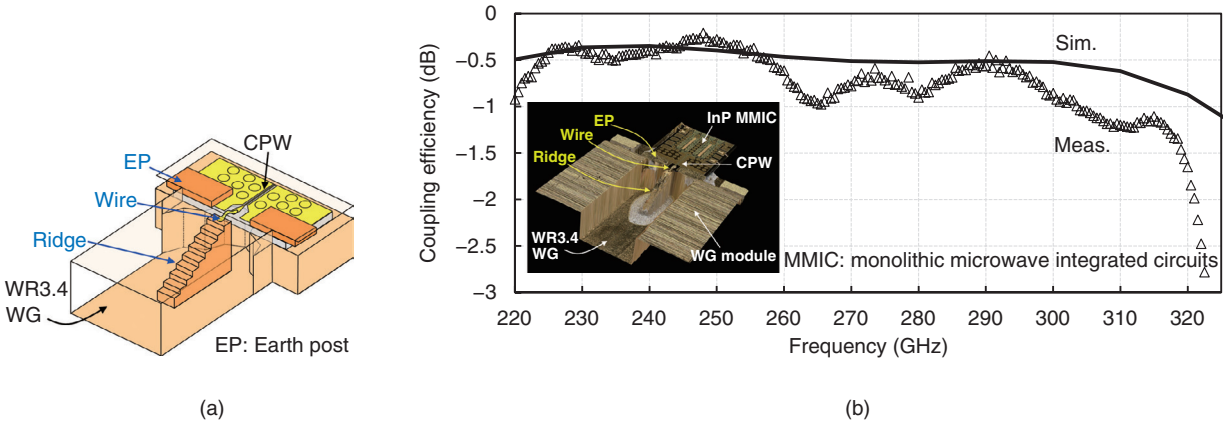

Fig. 6. (a) Schematic and (b) measured coupling efficiency of ridge coupler.

backside of the InP chip (**Fig. 5(b)**). Thus, the overlap between the RF TLs and wide DC lines in Fig. 5(a) is eliminated and the gain and output power of the PA increases. The simulation comparison of the PA gain is shown in **Fig. 5(c)**. By using the BDCL, the simulated gain increases by around 3 dB over 280–320 GHz.

The PA chip is difficult to handle for implementation in TRXs. To improve ease of handling, the IC packaging in a robust metal module is important. In the 300-GHz band, the widely used media is a rectangular waveguide (WG). Therefore, we developed a PA module with WG flanges for its input and output. The critical component for this PA module is the transition between the PA IC and WG. A ridge coupler [8, 9], shown in **Fig. 6(a)**, is used as the transition. It translates the guided mode of the WG to the coplanar waveguide (CPW) mode, which is used in the PA IC. A step-wise metal component formed on the center part of the WG, called a ridge, gradually transforms the impedance and forms of electromagnetic wave between the WG and CPW. A bondwire is used to connect the ridge and IC CPW pad. A three-dimensional photograph and simulated and measured coupling efficiencies of this ridge coupler are shown in **Fig. 6(b)**. The coupling loss is very small, less than 1 dB over 220–303 GHz.

The PA IC and module were fabricated using the techniques described above, as shown in **Figs. 7(a)** and **(b)**. The BDCL placed in the vicinity of the center part of the PA chip is electrically isolated from the DC ground by the mask and etching process in the InP back-end process, as shown in Fig. 7(a). The fabricated PA module has WR3.4-band (220–325 GHz) WG flanges for its input and output, as shown in Fig. 7(b).

The characteristics of the PA module were evaluated through small- and large-signal measurement. We first conducted a small-signal measurement using a vector network analyzer (VNA) and WR3.4-band frequency extenders. The measured S-parameters are shown in **Fig. 8**. It achieved a maximum gain (S_{21}) of 20.5 dB at 295 GHz and broad bandwidth. The reverse transmittance (S_{12}) is very small, less than

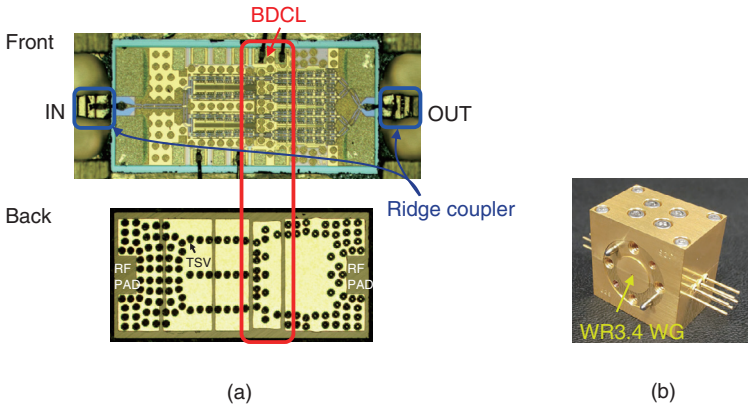

Fig. 7. Photographs of (a) 300-GHz PA chip and (b) module.

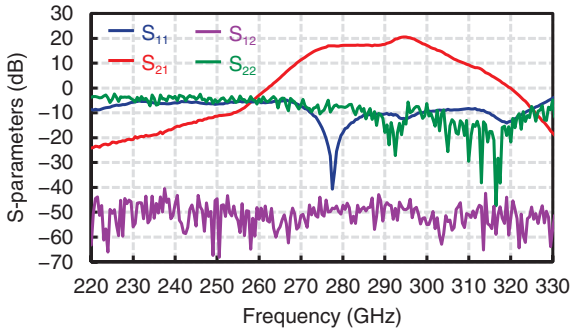

Fig. 8. Measured S-parameters of 300-GHz PA module.

–40 dB over the full WR3.4 band. Therefore, the PA module is very stable. This is because the InP back-end process shown in Fig. 3 successfully reduces substrate-mode propagation. The measured gain matches the simulated gain in Fig. 6(a).

Next, we measured large signal characteristics. The input-output characteristics are shown in **Fig. 9(a)**. The PA module achieved high saturated output power (Psat) and output 1-dB compression point (OP1dB) of 6 dBm. The measured frequency dependence of the Psat is shown in **Fig. 9(b)**. The Psat is larger than 10 dBm over 278–302 GHz. These high-power characteristics are derived from BDCL technique and the low-loss ridge coupler, as described above.

4. 300-GHz-band TRX

We fabricated a 300-GHz-band TRX using the PA module described in Section 3. The TRX has a heterodyne architecture. The transmitter (TX) consists of a frequency converter (mixer), local oscillation (LO) PAs to operate these mixers, and an RF PA (same as the one described in Section 3). The receiver (RX) is composed of a mixer, LO PA, and low noise amplifier (LNA). The intermediate frequency (IF) and LO frequency are set to 20 and 270 GHz, respectively. The fundamental mixer [8, 10] using our in-house InP-HEMT technology is used for both TX and RX. In the RX, the same PA discussed in Section 3 is used as the LNA. This TRX uses the upper-side band for the RF (290 GHz). High-gain (50 dBi) lensed horn antennas were used for both TX and RX in the wireless-transmission experiment discussed later. The lower-side band signal is cut by using the high pass filter (HPF), as shown in **Fig. 10**. Sixteen quadrature amplitude modulation (16QAM) is used as the modulation format for communication.

First, we conducted an experiment involving back-to-back data transmission. The TX and RX were directly connected through the attenuator (ATT) with

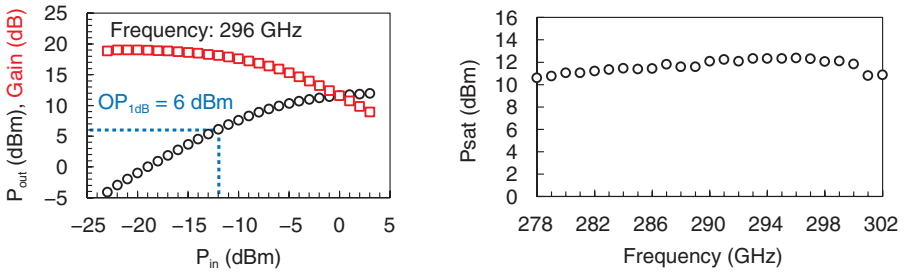

Fig. 9. Measured (a) input-output characteristics and (b) frequency dependence of Psat of 300-GHz PA module.

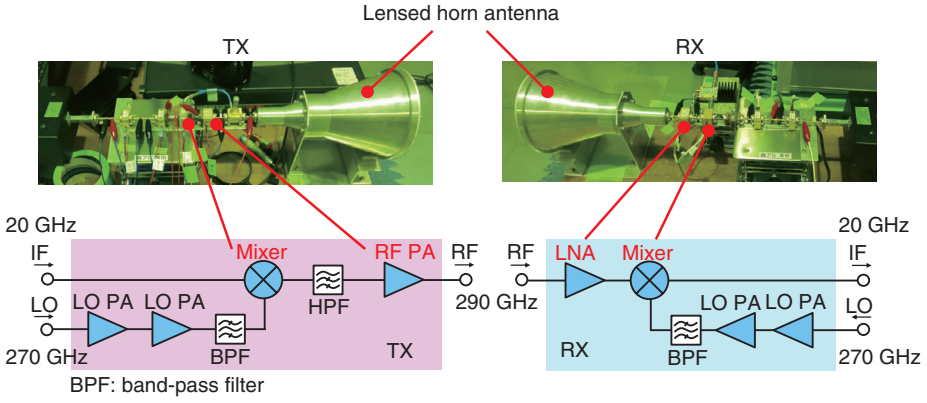

Fig. 10. Schematic and photograph of 300-GHz-band TRX.

attenuation of 9 dB. The role of this ATT is to protect the RX from the high output power of the PA. The SNR of the received IF signal was measured to evaluate the quality of communication. The SNR is related to the bit error rate (BER). The communication is judged successful when the measured SNR is larger than the required SNR (SNRreq), which is determined as the SNR where the corresponded BER is 10^{-3} in the following measurement. The SNRreq of 16QAM is 16.5 dB. The measured constellations and dependence of the baud rate with SNR of the received IF signal is shown in **Fig. 11**. As the frequency utilization efficiency of 16QAM is 4, the data rate is four times the baud rate. In the low baud rate region, the SNR is quite high, more than 25 dB. The SNR gradually degrades with the baud rate because the noise floor also increases with the increase in the baud rate. The maximum baud rate is 31 Gbaud, which corresponds to the very high data rate of 124 Gbit/s.

Next, we conducted an experiment involving wireless communication with the TRX with the 50-dBi lensed horn antennas described above. The link distance (TX antenna to RX antenna distance) was fixed to 9.8 m (**Fig. 12**). However, this link distance was virtually changed by changing the attenuation value of the variable ATT (VATT) inserted between the TX and TX antenna. This VATT equivalently adds the path loss between the TX and RX, and the path loss can be converted to the equivalent link distance. The measured SNR versus equivalent link distances of 15, 20, 25, and 30 Gbaud using the 16QAM signal are shown in **Fig. 13**. The high data rate of 120 Gbit/s (30 Gbaud) wireless transmission is successfully demonstrated. The received constellation of the 120 Gbit/s IF signal is also shown in Fig. 13. The maximum link distances, which are defined as the equivalent link distance where the SNR is the same as the 16QAM SNRreq, are 42, 29.5, 17.5, and 10.5 m for 15, 20, 25, and 30 Gbaud. The comparison of recently reported near-300 GHz TRX is shown in **Fig. 14**. The fabricated

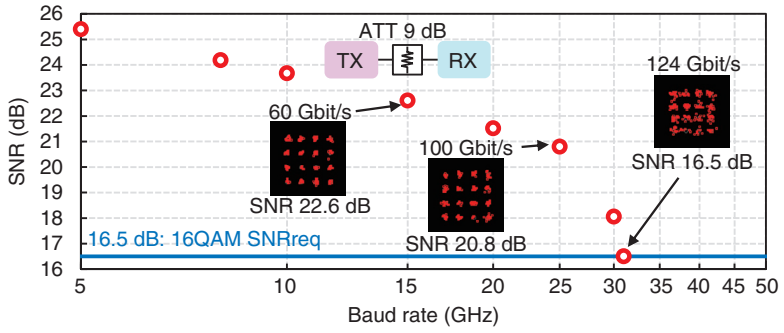

Fig. 11. Measured SNR vs. baud rate of 300-GHz-band TRX under back-to-back condition.

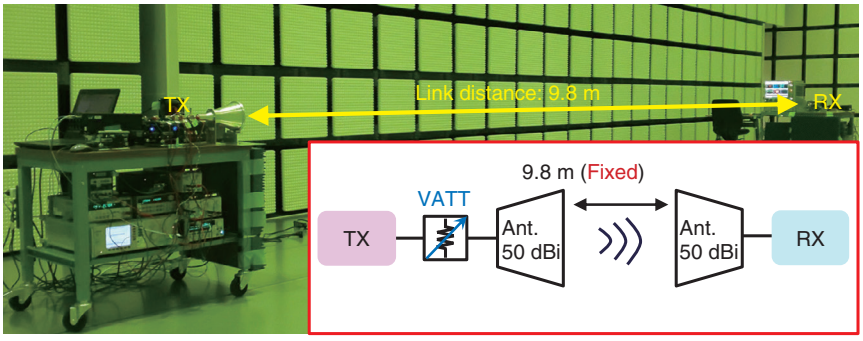

Fig. 12. Schematic and photograph of wireless-transmission experiment with 300-GHz-band TRX.

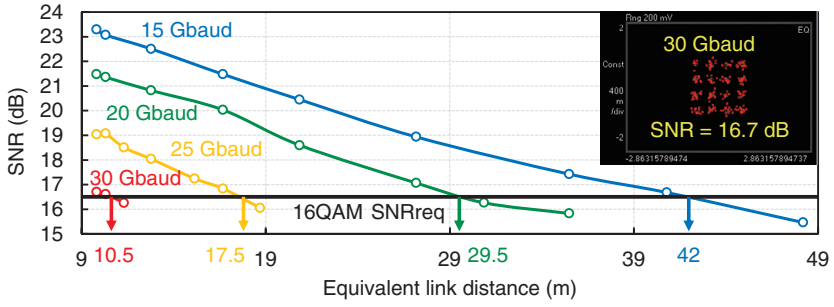

Fig. 13. Measured SNR vs. baud rate of 300-GHz-band TRX in 9.8-m wireless-communication experiment.

TRX shows the highest data rate among them.

5. Conclusion

We achieved 300-GHz-band 120-Gbit/s 9.8-m wireless transmission with a 300-GHz-band TRX using the high output power PA fabricated using our in-house InP-HEMT technology. The PA uses a special BDCL to lessen the RF loss and enhance its gain and output power. It achieves a maximum gain of 20.5 dB at 295 GHz, and Psat and OP1dB of 12 and 6 dBm at 296 GHz. The Psat is larger than 10 dBm for 278–302 GHz. The TRX was fabricated using the PA and our in-house 300-GHz fundamental mixer. It achieves a maximum data rate of 124 Gbit/s in 16QAM back-to-back data transmission. Wireless

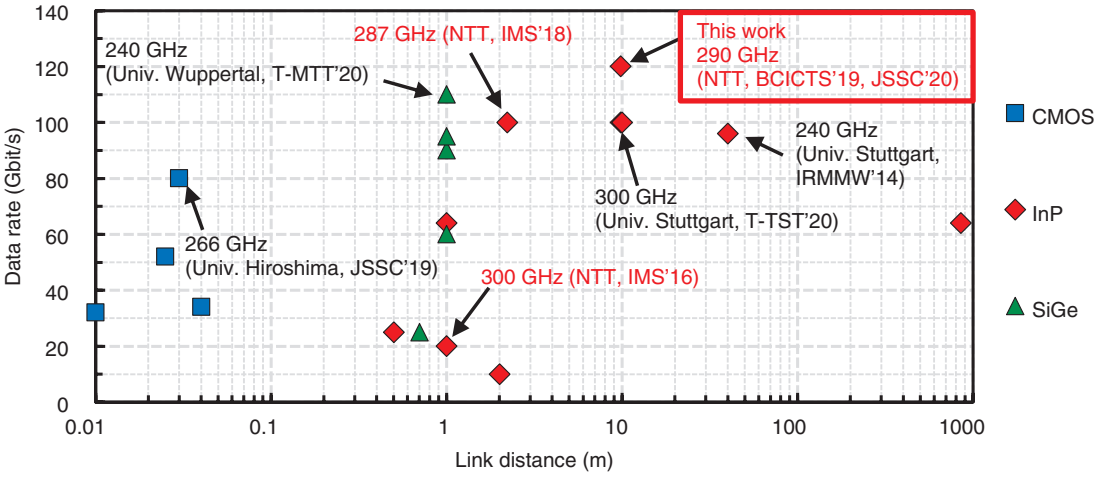

CMOS: complementary metal-oxide semiconductor
SiGe: silicon-germanium

Fig. 14. Plot of data rate and link distance for reported 300-GHz-band TRXs.

data transmission was successfully demonstrated with a link distance of 9.8 m for data rates of 60, 80, 100, and 120 Gbit/s using 16QAM. To the best our knowledge, the fabricated TRX achieves the highest data rate among the reported 300-GHz-band TRXs.

Acknowledgments

The authors wish to acknowledge Kenichi Okada of Tokyo Institute of Technology and Ho-Jin Song of NTT Device Technology Labs (now working at Pohang University of Science and Technology) for their fruitful discussions. We also thank the continuous assistant of Yukio Yago at NTT Electronics Techno Corporation. This work was supported in part by the Ministry of Internal Affairs and Communications, Japan, through the Research and Development Program for Expansion of Radio Resources.

References

[1] W. R. Deal, K. Leong, W. Yoshida, A. Zamora, and X. B. Mei, "InP HEMT Integrated Circuits Operating above 1,000 GHz," Proc. of IEEE International Electron Device Meeting (IEDM), San Francisco, CA, USA, Dec. 2016.

[2] H. Elayan, O. Amin, R. M. Shubair, and M. Alouini, "Terahertz Communication: The Opportunities of Wireless Technology Beyond 5G," Proc. of International Conference on Advanced Communication Technologies and Networking (CommNet), Marrakech, Morocco, Apr. 2018.

[3] P. Hillger, J. Grzyb, R. Jain, and U. R. Pfeiffer, "Terahertz Imaging and Sensing Applications with Silicon-based Technologies," IEEE Trans. Terahertz Sci. Technol., Vol. 9, No. 1, pp. 1–19, Jan. 2019.

[4] H. Sugiyama, H. Matsuzaki, H. Yokoyama, and T. Enoki, "High-electron-mobility $In_{0.53}Ga_{0.47}As/In_{0.8}Ga_{0.2}As$ Composite-channel Modulation-doped Structures Grown by Metal-organic Vapor-phase Epitaxy," Proc. of International Conference on Indium Phosphide and Related Materials (IPRM), Takamatsu, Japan, June 2010.

[5] H. Hamada, T. Tsutsumi, H. Sugiyama, H. Matsuzaki, H.-J. Song, G. Itami, T. Fujimura, I. Abdo, K. Okada, and H. Nosaka, "Millimeter-wave InP Device Technologies for Ultra-high Speed Wireless Communications toward Beyond 5G," Proc. of IEEE International Electron Device Meeting (IEDM), San Francisco, CA, USA, Dec. 2019.

[6] T. Tsutsumi, H. Hamada, K. Sano, M. Ida, H. Matsuzaki, "Feasibility Study of Wafer-level Backside Process for InP-based ICs," IEEE Trans. Electron Devices, Vol. 66, No. 9, pp. 3771–3776, Sept. 2019.

[7] H. Hamada, T. Tsutsumi, G. Itami, H. Sugiyama, H. Matsuzaki, K. Okada, and H. Nosaka, "300-GHz 120-Gb/s Wireless Transceiver with High-output-power and High-gain Power Amplifier Based on 80-nm InP-HEMT Technology," Proc. of IEEE BiCMOS and Compound Semiconductor Integrated Circuits and Technology Symposium (BCICTS), Nashville, TN, USA, Nov. 2019.

[8] H. Hamada, T. Tsutsumi, H. Matsuzaki, T. Fujimura, I. Abdo, A. Shirane, K. Okada, G. Itami, H.-J. Song, H. Sugiyama, and H. Nosaka, "300-GHz-Band 120-Gb/s Wireless Front-End Based on InP-HEMT PAs and Mixers," IEEE J. Solid-State Circuits, Vol. 55, No. 9, pp. 2316–2335, Sept. 2020.

[9] T. Kosugi, H. Hamada, H. Takahashi, H.-J. Song, A. Hirata, H. Matsuzaki, and H. Nosaka, "250–300 GHz Waveguide Module with Ridge-coupler and InP-HEMTIC," Proc. of IEEE Asia-Pacific Microwave Conference (APMC), pp. 1133–1135, Sendai, Japan, Nov. 2014.

[10] H. Hamada, T. Fujimura, I. Abdo, K. Okada, H.-J. Song, H. Sugiyama, H. Matsuzaki, and H. Nosaka, "300-GHz, 100-Gb/s InP-HEMT Wireless Transceiver Using a 300-GHz Fundamental Mixer," Proc. of IEEE MTT-S International Microwave Symposium (IMS), pp. 1480–1483, Philadelphia, PA, USA, June 2018.

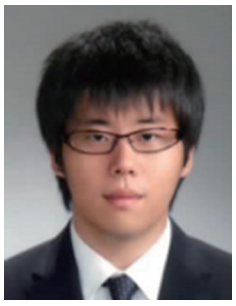

Hiroshi Hamada
Research Engineer, NTT Device Technology Laboratories.

He received a B.E. and M.E. in electrical engineering from Tokyo Institute of Technology in 2009 and 2011. He joined NTT Photonics Laboratories in 2011, where he started the research and development of the millimeter-wave/terahertz (MMW/THz) monolithic microwave integrated circuits (MMICs) for wireless communications. He is currently with NTT Device Technology Laboratories, where he is engaged in the research and development of THz MMICs for ultrahigh-speed wireless communications and THz imaging and sensing technologies. His research interests include MMW/THz IC design, package design, and device modeling of III–V transistors. Mr. Hamada is a member of the Institute of Electrical and Electronics Engineers (IEEE) and Institute of Electronics, Information and Communication Engineers (IEICE). He has been serving as a member for the IEEE Microwave Theory & Techniques Society (MTT-S) Technical Committee on Microwave and Millimeter-Wave Solid State Devices (MTT-9). He was a recipient of the IEEE International Microwave Symposium Best Industry Paper Award in 2016, the URSI (Union Radio-Scientifique Internationale) Asia-Pacific Radio Science Conference Young Scientist Award in 2016, the APMC (Asia-Pacific Microwave Conference) Prize in 2018, and the IEICE Young Researcher's Award in 2019.

Takuya Tsutsumi
Senior Research Engineer, NTT Device Technology Laboratories.

He received a B.E. in electrical engineering from Osaka City University in 2006, and an M.E. and Ph.D. in electronic engineering and informatics from Kyoto University in 2008 and 2018. In 2008, he joined NTT Photonics Laboratories. From 2013 to 2016, he was with NTT Access Network Service Systems Laboratories, where he was engaged in the development of optical network systems. He is currently with NTT Device Technology Laboratories, where he is involved in the research of InP-HEMT devices and the development of backside fabrication processes for high-speed ICs. He is a member of IEEE.

Hideaki Matsuzaki
Senior Research Engineer, Supervisor, NTT Device Technology Laboratories.

He received a B.S. and M.S. in physics from Kyoto University in 1993 and 1995, and a Ph.D. in engineering from Toyama University in 2019. He joined NTT Atsugi Electrical Communications Laboratories in 1995. He is with NTT Device Technology Laboratories, where he engages in research and development of compound semiconductor devices such as InP-HEMTs, HBTs, photodiodes, and laser-diodes. He is a senior member of IEEE, senior member of IEICE, and a member of the Institute of Electrical Engineers of Japan.

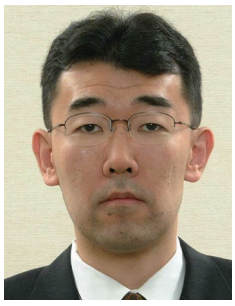

Hiroki Sugiyama
Distinguished Laboratory Specialist, Senior Research Engineer, NTT Device Technology Laboratories.

He received a B.S. and M.S. in physics from Tokyo Institute of Technology in 1991 and 1993. He joined NTT in 1993, where he has been engaged in research and development of epitaxial growth and characterization technology of III–V compound semiconductors for ultrahigh-speed electron devices. He is a member of the Japan Society of Applied Physics and the Physical Society of Japan.

Hideyuki Nosaka
Senior Research Engineer, Supervisor, Group Leader of High-Speed Analog Circuit Research Group, NTT Device Technology Laboratories.

He received a B.S. and M.S. in physics from Keio University, Kanagawa, in 1993 and 1995, and a Dr. Eng. in electronics and electrical engineering from Tokyo Institute of Technology in 2003. He joined NTT Wireless System Laboratories in 1995, where he was engaged in research and development of MMICs and frequency synthesizers. Since 1999, he has been with NTT Photonics Laboratories, where he has been involved in research and development of ultrahigh-speed mixed-signal ICs for optical communications systems. He is a member of IEICE and served as a TPC member for the IEEE CSICS from 2011 to 2013 and IEEE ISSCC from 2013 to 2017. He has been serving as a member for the IEEE MTT-S Technical Committee on RF/Mixed-Signal Integrated Circuits and Signal Processing (MTT-15). He was a recipient of the 2001 Young Engineer Award, the 2012 Best Paper Award presented by IEICE, and the APMC 2018 Prize.